BNL Experiment E949
Technical Note K-017

Downstream collar detector for E949

Yu. Kudenko, O. Mineev, N. Yershov
INR RAS, 60-th October Pr. 7a, Moscow 117312, Russia

J. Frank, E. Garber, S. Kettell, K. Li
Brookhaven National Laboratory, Upton, NY

June 5, 2001

1 Introduction

The collar detectors are placed just behind the CsI crystal detectors, around the beam channel. Upstream and downstream collars (CO) cover the fraction of solid angle (from $0.995 > \cos\theta > 0.97$) as a part of the E949 photon veto system. Their purpose is to detect photons emitted from the target under small polar angles. The old collars were "sandwiches" assembled of 25 layers of 5 mm thick plastic scintillator and 24 layers of 1 mm lead sheet, which have a total thickness of 4.6 radiation lengths (X_0). The light was readout of each sector through a set of curved Lucite light guides and a rectangular mixer block glued to the outer sandwich circumference. The light yield (l.y.) was measured with a muon beam at TRIUMF using the same readout configuration as in the experiment. The l.y. was found to be 29 p.e./MeV (where MeV is the visible energy deposit). GEANT simulation for a such sampling structure shows the detection inefficiency as high as 6–10% in photon energy range from 30 to 250 MeV with a detection threshold of 1 MeV ([1]). The main source of inefficiency is the escape of photons before conversion. The primary purpose of the CO upgrade is to enhance the photon detection efficieny by increasing the thickness of the detector, which allow E949 to fully exploit the capability of E949 and to reduce the $K_{\pi 2}$ background in the $\pi\nu\overline{\nu}2$ search. Fig. 1 illustrates the role of downstream CO for electromagnetic coverage in E949.

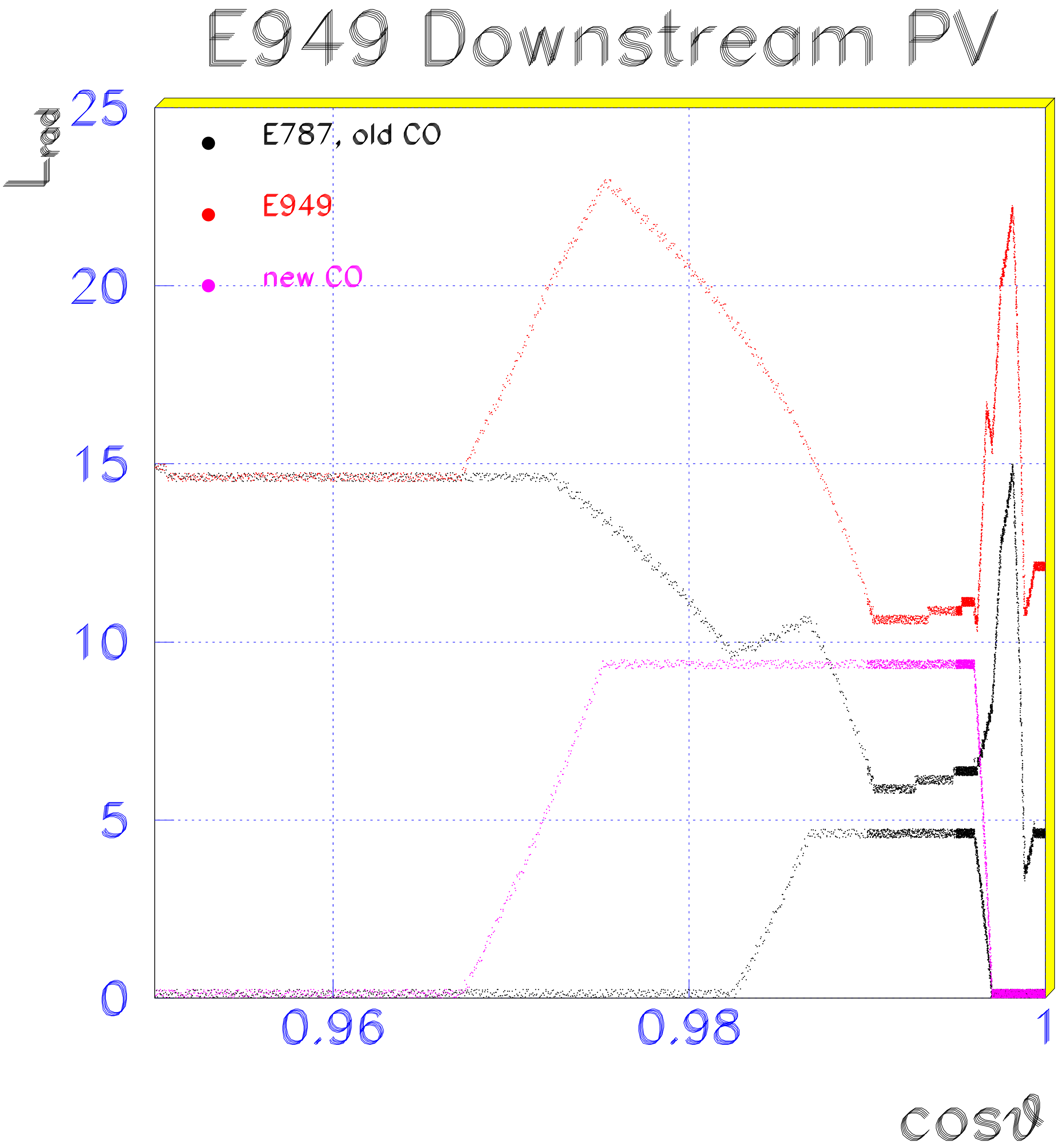

Figure 1: Radiation thickness of E949 in the forward direction.

2 Upgraded collar design

The assembly view of downstream CO is shown in Fig. 2 The upstream and downstream CO are similar in design, the difference is in the geometrical size. Accurate dimensions can be found at the website:
http://www.phy.bnl.gov/e949/detector/photon_veto/co/drawings.html.

The CO consists of 25 layers of 5 mm thick scintillator BC404(Bicron) and 24 layers of 2 mm lead absorber interleaved by 0.1 mm Tyvek reflector paper. The total radiation thickness is $\sim 9X_0$. GEANT simulation was done for a "sandwich" assembled of 26 layers of 5 mm scintillator and 25 layers of 2 mm thick lead (i.e. one layer more than for the real CO) [2]. The assembly dimensions were 14×14 cm^2 across, detection threshold was 1 MeV. The detection inefficiency was found to be 1.6% at photon energy of 40 MeV, and 0.9% at 100 MeV. Altough the real CO has smaller radiation thickness, its high light yield allow us to keep the detection threshold lower than 1 MeV increasing the detection efficiency.

A single plastic scintillator layer is segmented in 12 wedges (petals) forming 12 identical azimuthal sectors. Light from the petals is readout by WLS multi–clad fibers (BCF99-29AA from Bicron). A petal has 16 fibers glued in grooves in the BC404. One end of the fiber was polished and aluminized to provide a reflective mirror surface. All fibers for each sector ($16\times 25=400$) are terminated in a connector (see Fig. 3) which is coupled to a 46" Lucite rod via a silicone cookie. The rods transmit light to the phototubes in a low field region outside the magnet. Each lead layer is composed of two halves of 2 mm thick sheet (semi-disks). The Pb layers are laid out with a rotation angle of 30° relative to the neighboring layer providing coverage of the cracks between the Pb halves in subsequent layers. Since after γ-conversion in any point the electromagnetic shower will spread into the scintillator volume, there is no projective cracks for photons over a CO face. The cracks between scintillator petals are also staggered. The sandwich assembly is compressed between a base plate and an endplate disk (see Fig. 2) by 12 standoffs. The standoffs prevent the collar elements from shifting down out the assembly. All mechanical structure parts are made of Al except the standoffs, which are made of stainless steel.

The Al endplate facing the target is 6.3 mm thick ($0.07X_0$).

3 Construction and assembly

The BC404 sheets of 5 mm thickness and WLS fibers in 2 m long pieces were sent to Uniplast factory (Vladimir, Russia) from BNL. The petals were cut out of sheets with 0.1 mm tolerance. Since the scintillator sheet deviates from nominal thickness ± 0.2 mm (range from 4.8 to 5.2 mm), petals were hand selected in groups of similar thickness. The petals from the same group were laid out to form a single layer.

Sixteen symmetrically spaced grooves are cut along the petal with a saw blade which has an approximate U-shaped profile. Then the scintillator is etched by a chemical agent that results in the formation of a micropore deposit over the surface, following which the diffuse film is fixed in a settling tank. An advantage of this approach over the commonly used white diffuse papers is the almost ideal contact of the reflector with the scintillator. After etching a scintillator, including the groove surface, the white deposit inside the

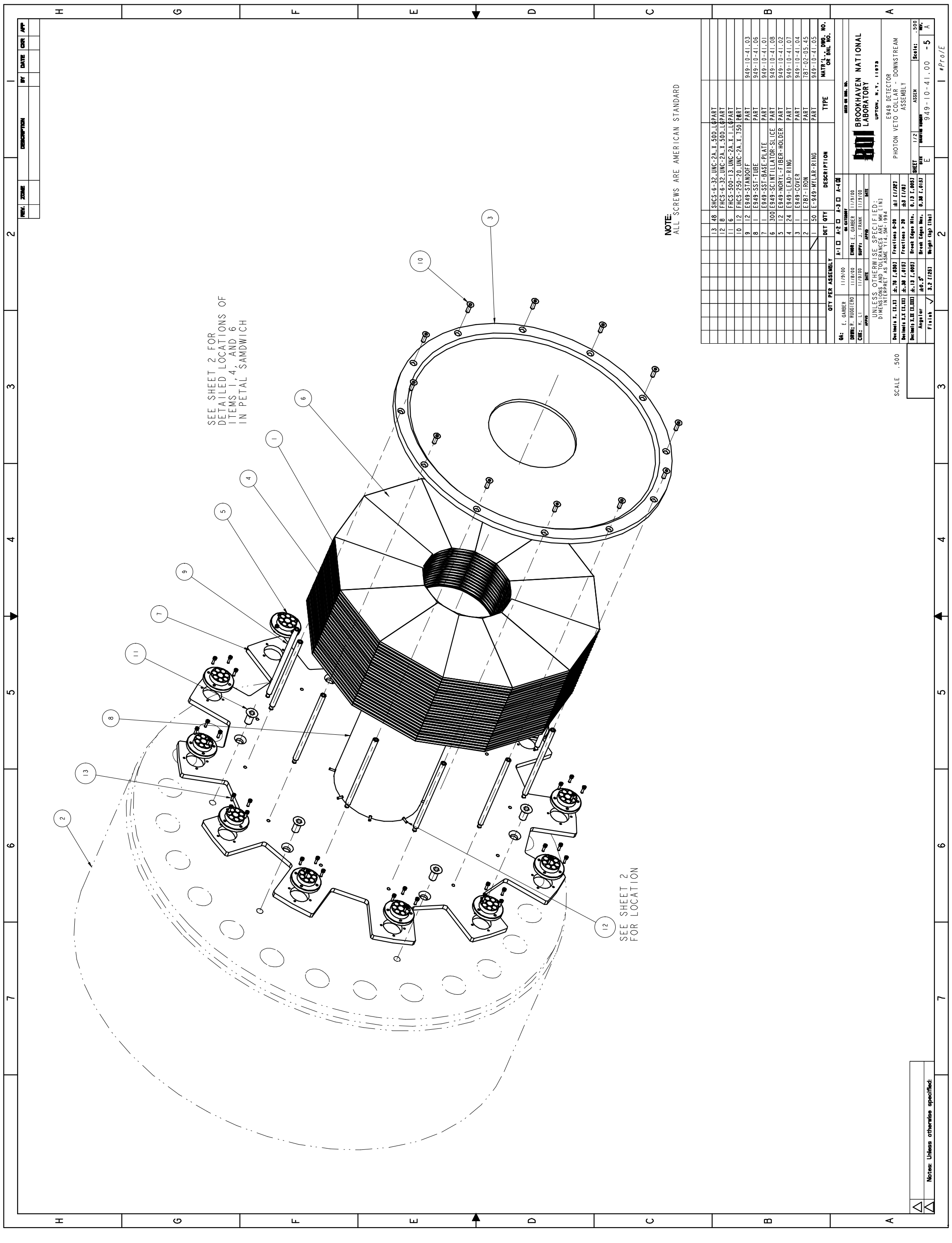

Figure 2: The assembly drawing of the downstream collar.

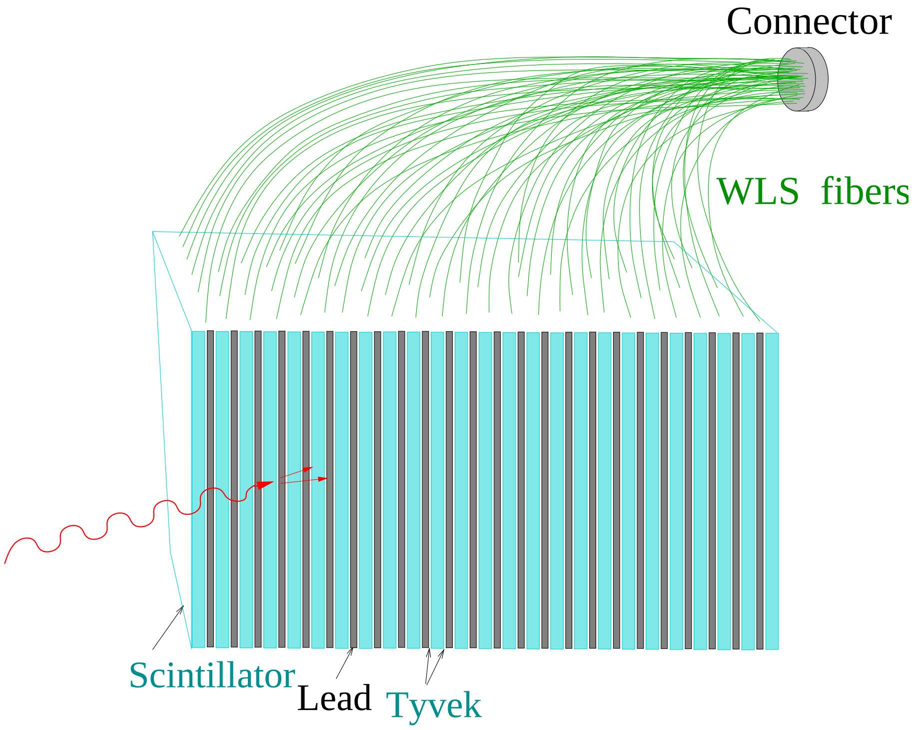

Figure 3: Schematic picture of one azimuthal sector.

grooves is removed by scraping along the groove profile. The scraping die also shapes the groove to the optimum U–shape cross–section. The groove depth is 1.2 mm. Polishing inside grooves is done by hand.

The WLS fibers were cut to a length of 65 cm. All fibers were tested because of fragility of the multi–clad BCF99-29 fiber. First, fibers were visually inspected, then they were bent over a cylinder with diameter of 5 cm to expose cracks. Failure rate (a fiber is broken) is below 0.5%.

Epoxy cement BC–600 (Bicron) provided the optical coupling between fibers and scintillator. Gluing was done in two steps. First, the grooves were filled with glue and the fibers were inserted. To accelerate hardening, the petals were heated to 40–45°C on the bench by an electrical film heater. In the second step, the glue was applied over the fibers to fill any remaining gaps.

Long term effect of Pb diffusion in the chemical reflector is unknown so Tyvek sheets were used to separate the scintillator and lead. The Tyvek also works as a diffuse reflector over the fibers.

The most critical point in collar assembling is the insertion of the fibers in the connectors. If fiber was bent with a radius of less than 3 cm, the crazing of the cladding was observed to develop (in the curved region) for some fibers. This process takes place in a hour and continues over 24–48 hrs. After that stabilization is observed (no additional crazing after ∼48 hours). The usual method to relax the bending stress is by heating. Due to the complicated readout configuration of the CO this method is not practical. Instead, the fibers were bent without heat, but with a radius of 4 cm or larger. Even so some fibers show crazing which is not harmful as long as the number of such fibers is

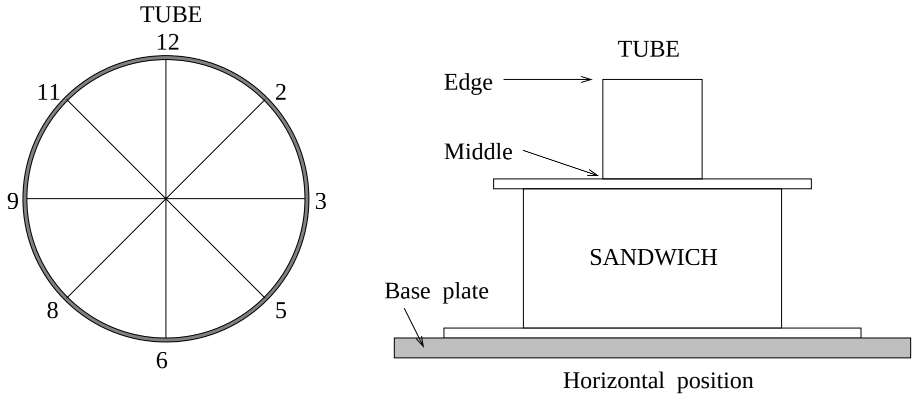

Diameter	Place	Horizontal position w/o base plate, in.	Vertical position with base plate, in.
12 − 6	Middle Edge	6.466 6.466	6.462 6.459
2 − 8	Middle Edge	6.468 6.472	6.472 6.477
3 − 9	Middle Edge	6.465 6.467	6.467 6.476
5 −11	Middle Edge	6.463 6.461	6.462 6.457

Figure 4: The tube diameter measured before and after the CO rotation. All dimensions in inches.

observed to be less than 1%. After fibers have been glued in a connector, the ends were cut and polished.

4 Mechanics

Deformation of mechanical assembly was checked by measuring the central tube diameter. If the whole assembly would be deformed after rotation of the detector from a horizontal orientation to a vertical one, the tube will change its shape under the weight of the detector (170 kg). Additional deviation may be introduced by mounting the CO to the main iron.

First, the tube diameter was measured in a few points while the CO rested horizontally on the bench. Then, the same measurements were repeated after the CO was attached to the heavy base plate and rotated to a vertical position (this is the orientation in the E949 detector). The base plate imitated the main iron. The measured tube diameters for both positions are listed in Fig. 4, where point #6 is the lowest one in the vertical position. The maximum change in the diameter is about 0.2 mm, that confirms mechanical rigidity of the detector.

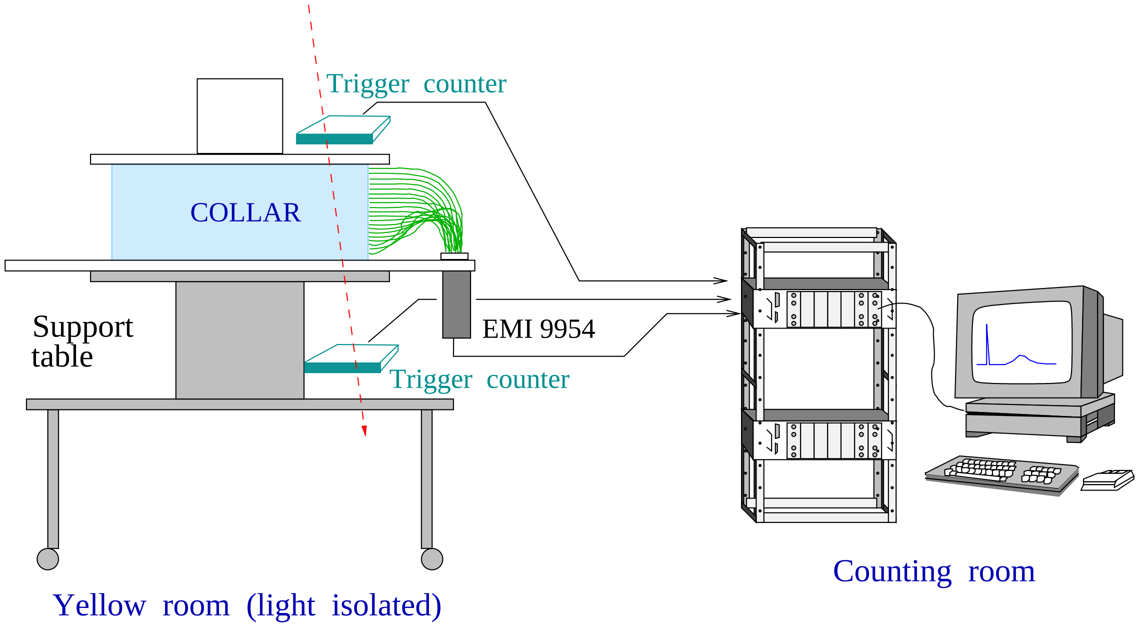

Figure 5: Cosmic test set–up.

5 Cosmic test

The collar was tested with cosmic rays as shown in Fig. 5. The trigger counters were placed above and below each sector. Though the area of the trigger counters is larger than that of a sector, the 50 cm separation selects minimum ionizing particles (MIP) with angles close to normal. A phototube is attached to the fiber connector through a silicone cookie. All sectors were measured with the same PMT. The detector was located in the "yellow" room, and signals were sent to the DAQ in room 1-86. The MIP signal is digitized by a LeCroy 2249A ADC. At first, measurements were started with a photomultiplier Thorn EMI-9821A (3" BV PMT). Then tests were continued with the 2" PMT Thorn EMI-9954 (effective cathode diameter is 46 mm), which will be actually used for CO readout. This phototube has a photocathode sensitivity extended in the green light region. Our results demonstrated that the EMI-9954 has 18-20% higher quantum efficiency (QE) for the green WLS light than the EMI-9821.

The average number of detected photoelectrons is calculated by dividing the MIP peak position by the single electron (SER) peak position. Measurement accuracy is determined mainly by the accuracy of SER calibration. Other factors include the optical contact with cookie and orientation of trigger counters. A MIP deposits about 25 MeV of visible energy in the collar, i.e. the signal amplitude is large enough to be out of SER range. Thus some scaling is required to match the small SER peak and large MIP peak, which is as large as 1000 photoelectrons. The ADC spectrum of SER was measured with a scintillator doped with ^{241}Am, which was observed by the 9954 in question as well as a trigger PMT. The scintillator was arranged such that the average light yield in the PMT under test was substantially less than 1 p.e. The scintillation light observed in the trigger PMT was used to gate the ADC for the PMT under test, so that the SER could be measured. The SER pulse was amplified with gain of 10. The MIP signal wass attenuated by a factor of 4.

Therefore, the scaling coefficient between MIP and SER peaks is 40. However, as shown in Fig. 6 the SER is unstable over time, so care had to be taken for the ~8 hour cosmic MIP runs. The SER calibrations are performed before and after each measurement, and an average between them is taken to calculate the number of p.e.

The results are presented in Fig. 7. Average yield is about 43 p.e./MeV, where MeV is visible energy. Deviation from this value in different sectors is ± 3 p.e., this is within the accuracy of the SER calibration.

Two sectors were tested with a 116 cm long lightguide attached between the PMT and the fiber connector (cookie on each end). The rod is the same one to be used for CO readout in the experiment. The rod attenuates light by about 40%, i.e. the l.y. for CO in the experiment is expected to be about 26 p.e./MeV.

6 Test with a radioactive source

To check the relative performance of the CO sectors we employed the ^{106}Ru-source, which emits electrons capable of penetrating through the 1.5 mm thick Al tube. The source is collimated by a 6 mm diameter aperture. This size was chosen to maximize the signal to background. The source was inserted inside the tube to irradiate the scintillator petals at the inner edges. The distance between the source and tube wall was about 2 cm, so a few layers were irradiated. The PMT anode current produced by the source is measured by a picoammeter. Characteristic numbers are: 620 nA with the source, 130 nA without the source. The response of each sector to irradiation is shown in Fig. 8. The lightguide attenuates the current by 35% in average, that is consistent (or even more optimistic than) with the cosmic ray measurements. The light output of each sector is the same within the measurement accuracy. The measurement accuracy depends on the quality of optical contact and, to larger degree, the photocathode non-uniformity. The last effect is described below.

The 9954 PMT used for the measurements has rather strong non-uniformity of the photocathode sensitivity. This effect was measured using the "separated fiber readout". As shown in Fig. 9, the fiber connector has 8 holes of 8 mm diameter, where the whole fiber bundle is separated into 8 groups. Each group combines the fibers from a few neighboring layers. The source was positioned to irradiate the first layers of a sector, which are readout through the fibers marked by green in Fig. 9. After each measurement the phototube was rotated by 45°. In such a way the light spot of 8 mm diameter moves on a circle of 24 mm diameter. The sensitive photocathode area has 46 mm diameter. Optical coupling was provided by a cookie. The measurements were repeated twice, and the average values are plotted in Fig. 10. The curve indicates a large degree of photocathode non-uniformity. The tests were performed only with one PMT, thus it is not clear if a such nonuniformity is an individual or common feature for the EMI-9954. In the experiment the long lightguide rods will work as a mixer to distribute light over the photocathode more uniformly.

7 Tests after collar installation

After the downstream collar was installed and the lightguide rods were mounted, the test with the radioactive source was repeated. All sectors were viewed by the same phototube. The optical contact between the rod and fiber connector is provided by a cookie. The

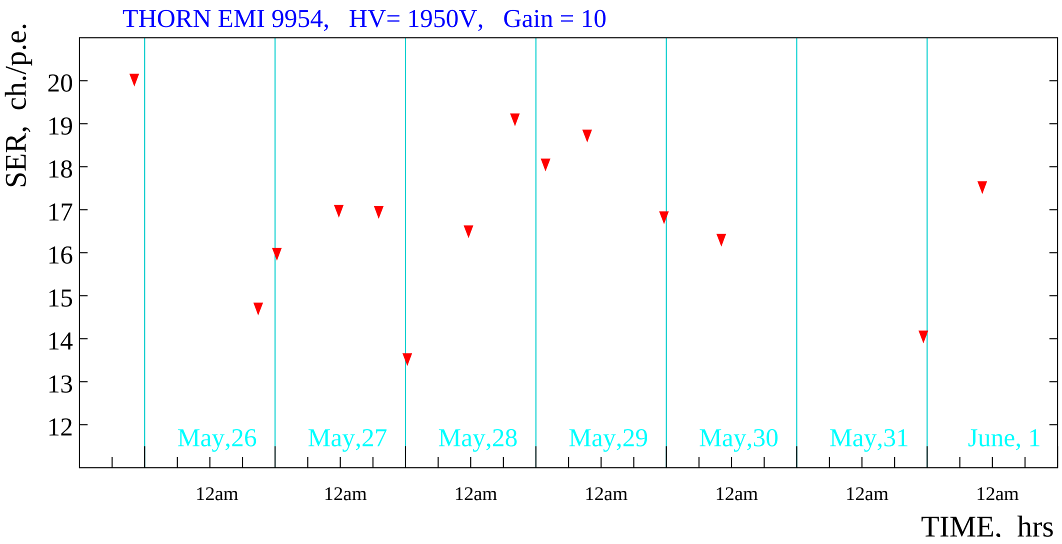

Figure 6: SER amplitude of an EMI-9954 phototube measured over 7 days.

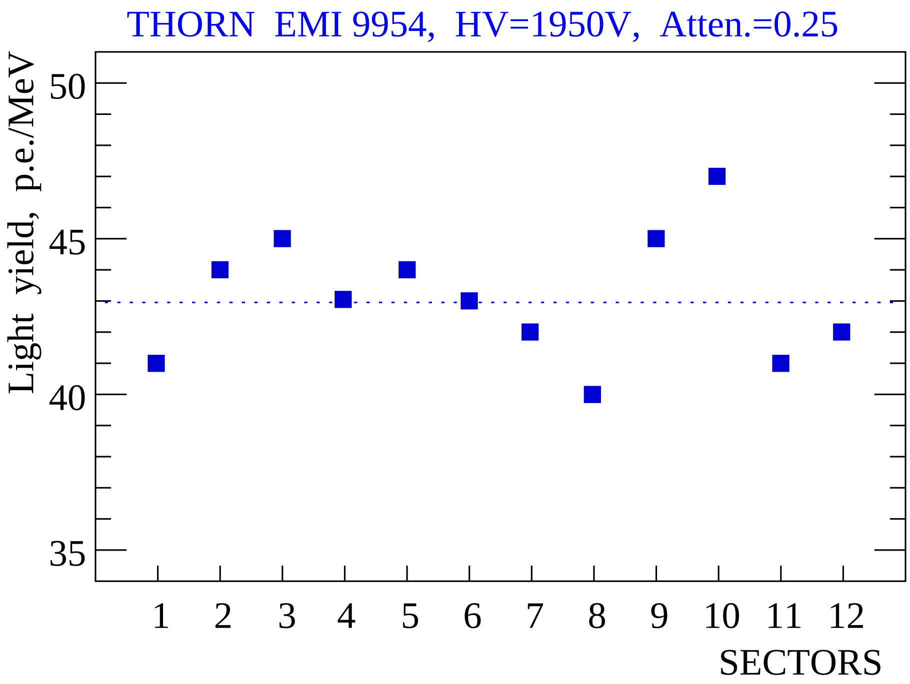

Figure 7: Light yield of the downstream collar for each sector, measured with cosmic rays. Direct fiber readout with PMT with no lightguide rod.

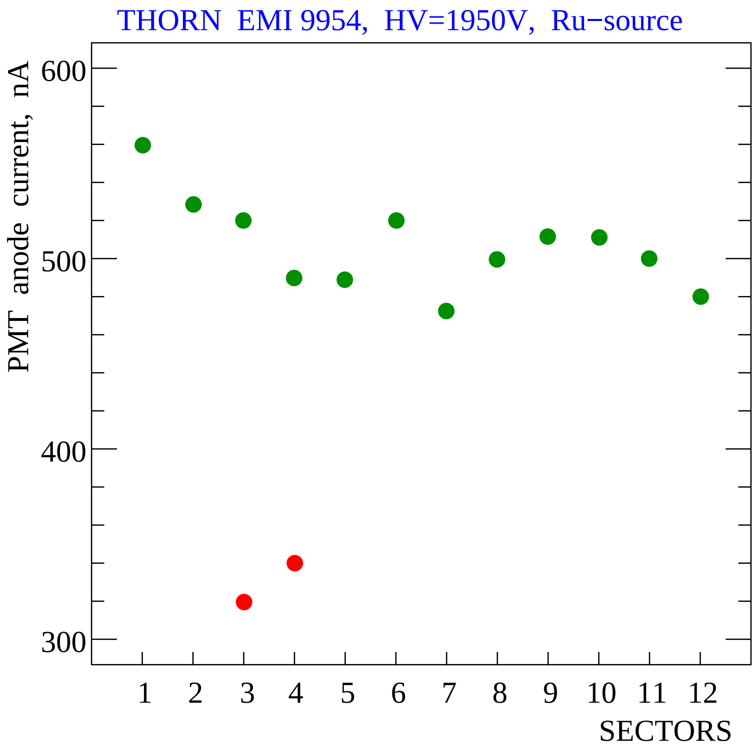

Figure 8: The PMT anode current measured with a picoammeter for each sector irradiated by the ^{106}Ru source. The background current (source out) is subtracted. Red circles indicate the current with the lightguide installed.

phototube had an air contact with the rod. The distribution of sector responses is shown in Fig. 11, where the results for a direct contact of the phototube with the fiber connector are also shown. The source positions were different for the both cases, therefore the current reduction can not be applied to calculate the rod attenuation. From Fig. 11 light variation from sector to sector is within 21%, while before installation it was 18%. This increase may have been introduced by the rods and optical couplings. Nevertheless, uniformity of response testifies to the stablity of the collar performance after installation.

All collar phototubes were checked by measuring their SERs with ^{241}Am-pulser. PMTs show good SER peaks except the 3-d tube, which was replaced by the spare one. Although the low SER is not a defect, it could be an evidence of malfunction. The results of measurements are listed in Table 1. The SER amplitudes reflect the phototube gains, which can be adjusted by HV power supply.

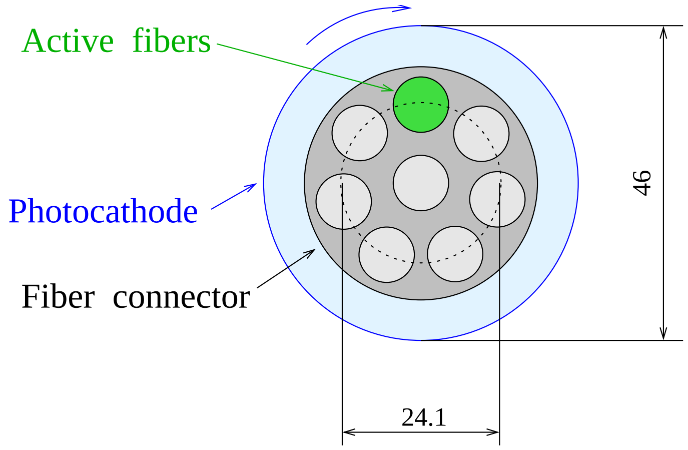

Figure 9: The test of the uniformity of photocathode sensitivity. Only fibers in the "green" hole (active fibers) produce light from the source illumination of the scintillator, other fibers produce background light.

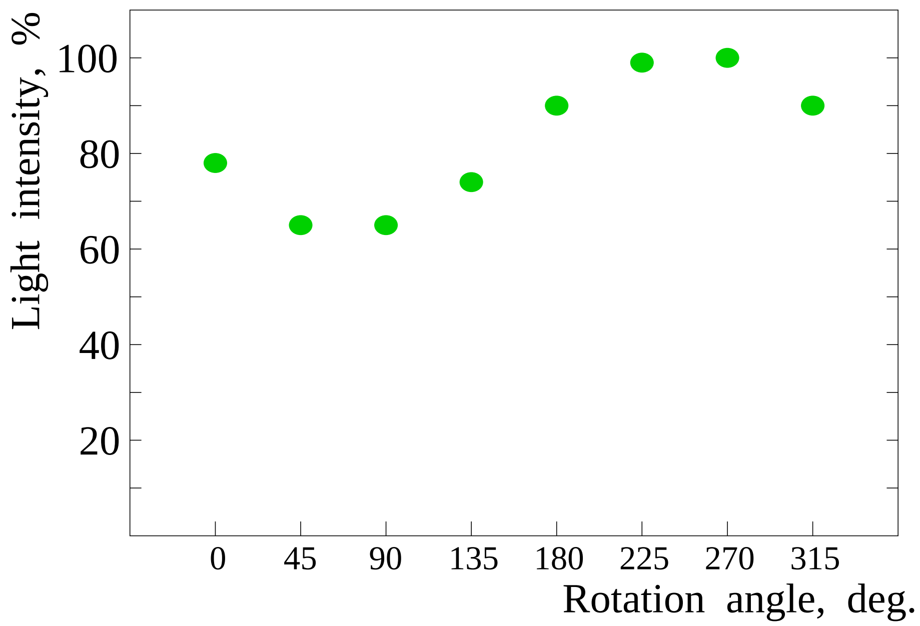

Figure 10: The relative light intensity dependence on the light source position over the photocathode. The light intensity is measured by anode current. Background light (no source) is subtracted.

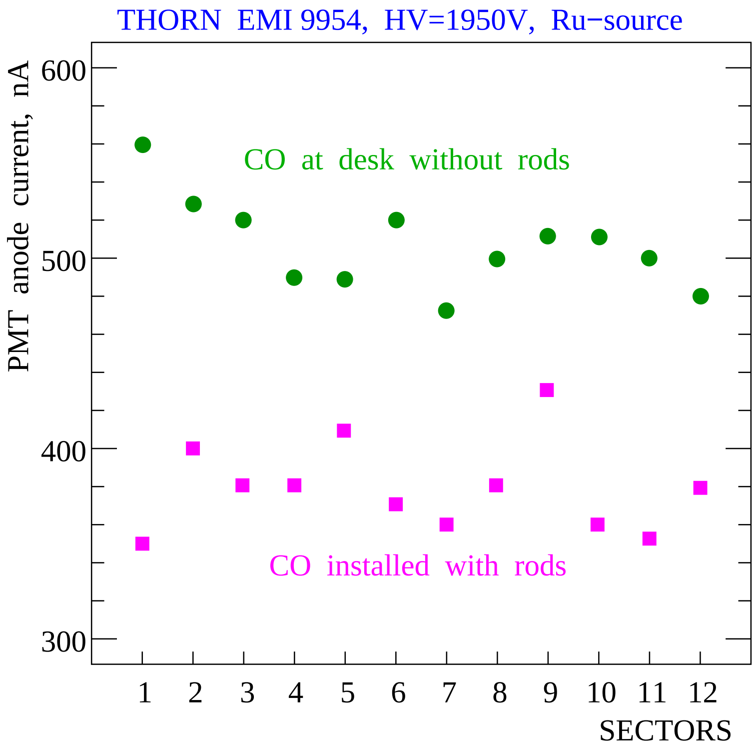

Figure 11: The PMT anode current measured in different sectors before and after collar installation. The background current is subtracted.

Table 1: SER amplitudes for the PMTs used for the collar.

Phototube	1	2	3	4	5	6	7	8	9	10	11	12
SER, ADC counts	124	52	22	74	53	74	118	144	45	92	61	111

8 Summary

The new collar detector is a Pb–scintillator sandwich, like the old collar, but with WLS fiber readout. Radiation thickness is a factor of two larger at $9X_0$. The expected light yield is about 26–28 p.e./MeV(visible). While having comparable light yield, the new collar is 2 times thicker than the old one in terms of radiation lengths. This thickness reduces the detection inefficiency for 100 MeV photons from 7% to 0.9% at the detection threshold of 1 MeV. In lower energy range ($E_\gamma < 30$ MeV) the inefficiency is dominated by sampling fluctuations, which are larger for the new collar. However, low energy γ constitute a relatively small fraction of the whole range. The downstream CO closes the hole in the solid angle for photons emitted from the target (particularly for pnn2). The hermetic electromagnetic coverage in E949 allow us to increase the sensitivity to search $K^+ \to \pi^+ \nu \bar{\nu}$ decays.

References

[1] V. Kurshetsov, A Simulation of the E949 Collar Detector using GEANT, E949 technote K-019.

[2] I. Britvitch, GEANT study for the Collar counter, technote.